Mechanisms of Stabilization of the Insulin Hexamer through Allosteric Ligand Interactions†

Sophie Rahuel-Clermont,‡ Cherie A. French,‡ Niels C. Kaarsholm,§ and Michael F. Dunn*,‡

Department of Biochemistry-015, University of California at Riverside, Riverside, California 92521-0129, and Novo Research Institute, Novo Nordisk A/S, Novo Allé, 2880 Bagsværd, Denmark

Received December 11, 1996; Revised Manuscript Received March 14, 1997⊗

ABSTRACT: The insulin hexamer is an allosteric protein capable of undergoing transitions between three conformational states: T_6, T_3R_3, and R_6. These transitions are mediated by the binding of phenolic compounds to the R-state subunits, which provide positive homotropic effects, and by the coordination of anions to the bound metal ions, which act as heterotropic effectors. Since the insulin monomer is far more susceptible than the hexamer to thermal, mechanical, and chemical degradation, insulin-dependent diabetic patients rely on pharmaceutical preparations of the Zn−insulin hexamer, which act as stable forms of the biologically active monomeric insulin. In this study, the chromophoric chelator 2,2′,2″-terpyridine (terpy) has been used as a kinetic probe of insulin hexamer stability to measure the effect of homotropic and heterotropic effectors on the dissociation kinetics of the Zn^{2+}− and Co^{2+}−insulin hexamer complexes. We show that the reaction between terpy and the R-state-bound metal ion is limited by the $T_3R_3 \rightleftharpoons T_6$ or $R_6 \rightleftharpoons T_3R_3$ conformational transition steps and the dissociation of one anionic ligand, or one anionic ligand and three phenolic ligand molecules, respectively, for T_3R_3 and R_6. Consequently, because the activation energies of these steps are dominated by the ground-state stabilization energy of the R-state species, the kinetic stabilization of the insulin hexamer toward terpy-induced dissociation is linked to the thermodynamic stabilization of the hexamer. The mass action effect of anion binding and, foremost, of phenolic ligand binding provides the major mechanism of stabilization, resulting in the tightening of the tertiary and quaternary hexamer structures. Using this kinetic method, we show that the R_6 conformation of Zn−insulin in the presence of Cl^- ion and resorcinol is >1.5 million-fold more stable than the T_3 units of T_6 and T_3R_3 and >70 000-fold more stable than the R_3 unit of T_3R_3. Furthermore, the stabilization effect is correlated with the affinity of the ligands: the tighter the binding, the slower the reaction between terpy and R-state-bound metal ion. These concepts provide a new basis for the pharmaceutical improvement of the physicochemical stability of formulations both for native insulin and for fast-acting monomeric insulin analogues through ligand-mediated allosteric interactions.

Since its introduction for treatment of insulin-dependent (type 1) diabetes mellitus (IDDM)[1] in the 1920s (Banting & Best, 1922), the allosteric properties of the Zn^{2+}−insulin hexamer have been used (albeit unknowingly) in the formulation of pharmaceutical preparations. This occurred through the use of auxiliary substances such as phenolic compounds (phenol, *m*-cresol, and methylparaben) added as antimicrobial preservatives and of anions (chloride and acetate) employed as isotonic agents (Brange et al., 1987). During the development of the various formulations currently in use, these additives were found to influence the physical state and physicochemical stability of insulin, suggesting more specific interactions with the protein (Brange & Langkjær, 1993).

The mechanisms underlying these effects have been uncovered by structural and functional analyses of the insulin hexamer in both the crystal and solution states. X-ray crystallography studies (Blundell et al., 1972; Bentley et al., 1976; Smith et al., 1984; Baker et al., 1988; Derewenda et al., 1989; Smith & Dodson, 1992a,b; Ciszak & Smith, 1994; Smith & Ciszak, 1994; Whittingham et al., 1995) have identified three different states of the zinc-protein complex, designated T_6, T_3R_3, and R_6 (Kaarsholm et al., 1989), which consist of two interdigitated T_3 and/or R_3 trimeric units (Figure 1). In the T state, the eight residues of the B chain N terminus assume an extended conformation (Figure 1a), whereas these residues are folded into an α-helix in the R state (Figure 1b), thereby opening hydrophobic pockets located at the dimer−dimer interfaces within the hexamer (Figure 1e). These sites accommodate a variety of small organic molecules such as *phenols*. Two Zn^{2+} ions reside on the 3-fold axis of the structure (Figure 1a,b), coordinated by the three symmetry-related HisB10 residues from each

† This work was supported by a gift from the Novo Research Institute.

* To whom correspondence should be addressed. Telephone: (909) 787-4235. Fax: (909) 787-3590.

‡ University of California at Riverside.

§ Novo Nordisk A/S.

⊗ Abstract published in *Advance ACS Abstracts,* May 1, 1997.

[1] Abbreviations: IDDM, insulin-dependent diabetes mellitus; In, insulin monomer; A^-, anionic ligand; M^{2+}, Zn^{2+} or Co^{2+}; P, phenolic ligand; T and R, insulin monomer forms with extended (T) and α-helical (R) conformations of B chain residues 1−8; T_6, T_3R_3, and R_6, three general conformations of the insulin hexamer; Co^{2+}/Co(II)−insulin, Zn^{2+}−insulin, and Zn^{2+}−T_6, cobalt- and zinc-substituted insulin hexamer complexes; T_3 and R_3 unit, T-state and R-state trimeric units of T_6, T_3R_3, and R_6; $\Delta G^{\ddagger}(T_3R_3)$ and $\Delta G^{\ddagger}(R_6)$, activation energies of the rate-limiting steps for the reaction between terpy and the R_3 units of T_3R_3 and R_6, respectively; *L*, allosteric constant calculated as [T state]/[R state]; K_d^R, dissociation constant of a phenolic ligand from the R-state phenolic pocket; $K_d^{R_3}$, dissociation constant of an anionic ligand from the R_3 unit metal coordination site; terpy, 2,2′,2″-terpyridine; Tris, tris(hydroxymethyl)-aminomethane.

S0006-2960(96)03038-3 CCC: $14.00

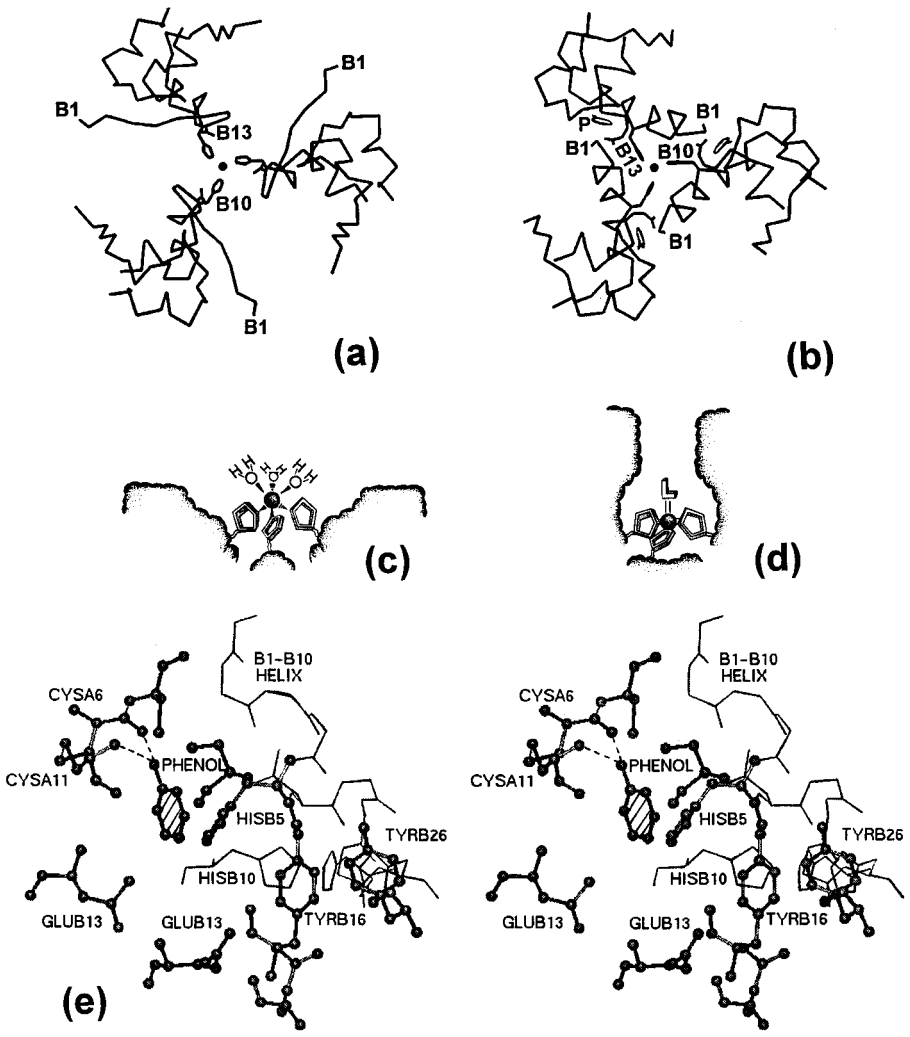

FIGURE 1: α-Carbon tracings of a T_3 unit (a) and an R_3 unit (b) taken from the X-ray structures of the T_6- and R_6-insulin hexamers (Baker et al., 1988; Derewenda et al., 1989) are viewed along the 3-fold axes of symmetry. In T_3, residues 1−9 of the B chain have an extended conformation (a); in R_3, these residues take up an α-helical conformation. Insulin hexamers consist of two interdigitated trimers, and to a first approximation, two T_3 units combine to give T_6, a T_3 unit and an R_3 unit combine to give T_3R_3, and two R_3 units combine to give R_6. The locations of the phenolic pockets in panel b (with phenol bound) are indicated by the symbol P. In cartoons c and d the HisB10 Zn^{2+} sites of the T state (c) and the R state (d) are viewed perpendicular to the 3-fold symmetry axis. In the T state (c), the octahedral ligand field about Zn^{2+} consists of three HisB10 side chains and three water molecules. In the R state (d), the tetrahedral ligand field of Zn^{2+} consisting of the three HisB10 side chains and a fourth (exogenous) ligand. In panel e, a stereodiagram of the phenolic pocket of an R_6 site is shown with phenol (striped structure) shown hydrogen bonded to CysA6 and CysA11. The phenolic binding pockets are located at the dimer−dimer interface, viz. panel b, in both the R_6 (six sites) and the T_3R_3 (three sites) conformations. The drawings in panels a−d are taken from Bloom et al. (1995). Copyright 1995 Academic Press. The drawing in panel e is taken from Choi et al. (1996). Copyright 1996 John Wiley & Sons.

trimeric unit. During the T to R conformational transition, the packing of the B1−B8 helical segments causes the Zn^{2+} coordination geometry to switch from an octahedral arrangement open to the solvent (Figure 1c), consisting of three HisB10 nitrogens and three water molecules, to a tetrahedral or five-coordinate arrangement located at the bottom of a narrow tunnel where a single anion such as chloride, phenolate, organic carboxylates, or thiocyanate (A^-) replaces the three water molecules (Figures 1d and 4). Solution studies from our laboratory (Palmieri et al., 1988; Kaarsholm et al., 1989; Brader et al., 1991; Choi et al., 1993, 1996; Brzovic et al., 1994; Bloom et al., 1995) and from others (Renscheidt et al., 1984; Wollmer et al., 1987; Krüger et al., 1990; Jacoby et al., 1993; Birnbaum et al., 1996) have shown that the allosteric behavior of the insulin hexamer arises from a preexisting set of equilibria between the three conformations ($T_6 \rightleftharpoons T_3R_3 \rightleftharpoons R_6$) that are driven toward T_3R_3 and R_6 by the binding of *phenolic compounds* to the R-state hydrophobic pockets. Binding to these sites (three in T_3R_3 and six in R_6) provides homotropic allosteric effects. Furthermore, the binding interactions at the phenolic pockets act synergistically with the binding of certain *anions* to the R_3 subunit zinc ions, giving rise to heterotropic allosteric effects that also stabilize T_3R_3 and R_6 (Brader et al., 1991; Choi et al., 1993, 1996). Therefore, in most pharmaceutical preparations, the insulin conformations with enhanced physicochemical stability consist of T_3R_3 and/or R_6 species.

The insulin monomer is far more susceptible than the hexamer to thermal and mechanical (fibrillation) denaturation as well as chemical degradation, including deamidation, disulfide bridge cleavage, and covalent dimerization by reaction of the B chain amino terminus with Asn or Gln residues. Therefore, hexamer stability regulates insulin shelf life (the maximum recommended storage time is currently 2 years for native human insulin; Brange & Langkjær, 1993), biological activity, immunogenicity, and potential sensitivity

to proteolytic degradation in the subcutaneous interstitial space after injection (Brange et al., 1987; Brange & Langkjær, 1993). Furthermore, the challenge of the insulin-replacement treatment in type 1 diabetics consists in reproducing the complex pattern of insulin secretion dynamics in healthy individuals, to achieve a strict homeostasis of glycemia in both basal and meal-related situations (Brange et al., 1990). Recent research has focused on the design of new insulin species with improved action profiles such as the "monomeric" insulin mutants which are rapidly taken up into the blood stream after subcutaneous injection (Brange et al., 1990), and at least one such "fast-acting" insulin mutant is presently on the market. While these genetically engineered insulins show improved response times and action profiles, they have proven to be much more difficult to stabilize than native human insulin (Brems et al., 1992a). This instability is a consequence of the reduced tendency to undergo aggregation and potentially compromises their usefulness (Brange et al., 1990; Brems et al., 1992b). Therefore, the stability to dissociation of both the native and engineered insulin hexamers is a parameter of utmost importance in optimizing insulin-replacement therapy.

Empirical research achieved considerable success in designing formulations with gradually increased physicochemical stability and slower action profiles, preparations well-suited to compensate for the basal requirements for insulin while sparing diabetics the discomfort of multiple daily injections. The principle governing these developments was the modulation of the physical state and the solubility of insulin (soluble, amorphous precipitate, or crystalline) and the use of additives such as protamine (Brange et al., 1987).

In this study, we explore the idea that the stability[2] of the insulin hexamer can be modulated by the nature and the concentration of its allosteric ligands. We have used the chromophoric chelator 2,2″,2″-terpyridine (terpy) as a kinetic probe to measure the effects of homotropic and heterotropic effectors on the terpy-induced dissociation kinetics of the Zn^{2+}− and Co^{2+}−insulin hexamer complexes (Dunn et al., 1980; Storm & Dunn, 1985; Kaarsholm et al., 1989). It will be shown that the rate-limiting step of this reaction depends on both the conformation and the ligation state of the insulin hexamer. Therefore, the effects of conformation and ligand binding on the stability[2] of each species of hexamer against the terpy-induced dissociation have been quantified. We show that the tighter tertiary and quaternary structures of the R-state species cause the R_6 conformation to be more stable than T_3R_3 and T_6 by several orders of magnitude. This effect is strictly correlated to the affinity of the ligands and is enhanced by the concerted effects of the T ⇌ R conformational transition and the mass action of ligand binding. The concepts arising from this study provide new strategies for the necessary physicochemical stabilization of the formulations both for native insulin and for fast-acting monomeric insulin analogues.

[2] Hereafter, unless otherwise stated, "stability" refers to the stability of the insulin hexamer−metal complex with respect to the terpy-induced dissociation, as measured by the rate of reaction between terpy and the HisB10 metal ions. It is argued herein that the kinetic dependencies of this reaction reflect properties of the T_6, T_3R_3, and R_6 insulin hexamers consisting of a combination of kinetic lability and thermodynamic stability.

MATERIALS AND METHODS

Materials. The chemicals employed in this study were reagent grade or better and were used without further purification. Metal-free human insulin was a gift supplied by Novo Nordisk (Bagsværd, Denmark). Phenol was purchased from Aldrich. Tris base, resorcinol, 2,2′,2″-terpyridine (terpy), and zinc sulfate were purchased from Sigma. Perchloric acid and potassium thiocyanate were purchased from Mallinckrodt. Potassium chloride was purchased from Fisher Scientific. Cobalt perchlorate was purchased from Alfa Products.

Methods. All experiments were carried out in 50 mM Tris/$HClO_4$ buffer at pH 8.0. The concentrations of insulin monomer and terpy stock solutions were determined from absorbance measurements using molar extinction coefficients of $\epsilon_{280} = 5700\ M^{-1}\ cm^{-1}$ (Porter, 1953) and $\epsilon_{290} = 16\,000\ M^{-1}\ cm^{-1}$ (Holyer et al., 1966), respectively. The metal ion content of insulin stock and metal ion stock solutions was assayed by titrations with terpy measured at the appropriate maximum absorbance wavelength of $M^{2+}(terpy)_2$ complexes (Holyer et al., 1966; Pattison & Dunn, 1976; Storm & Dunn, 1985).

Metal-substituted insulin hexamers were prepared by addition of the metal ion of choice to buffered solutions of metal-free insulin just prior to use, at the stoichiometry of 1.2 metal ions per hexamer in order to maximize binding of the metal to insulin. When needed, the other ligands were added to the insulin solution in the order anion and then phenolic ligand. To ensure pseudo-first-order kinetics, the reaction was initiated by mixing a solution of terpy with the insulin solution at a final concentration of 500 μM, a concentration in great excess compared to the metal ion concentration. The appearance of both the $Zn(terpy)_2^{2+}$ and the $Co(terpy)_2^{2+}$ complexes was followed at 334 nm, where the contribution of free terpy is negligible compared to the amplitude of the observed processes. The disappearance of R-state Co^{2+}−insulin species was followed by changes in the d−d transition spectrum of the anion−Co(II)−insulin complexes at 600 nm, where the contribution of the $Co(terpy)_2^{2+}$ complex is not significant.

Electronic spectra and slow kinetics (longer than 10 min) were recorded on a Hewlett-Packard 8452A diode array spectrophotometer. Single-wavelength, rapid-mixing kinetics (a total duration of less than 600 s) were performed on an Applied Photophysics SFMV17 mixing unit equipped with a 1 cm light path observation cuvette and customized optical and data acquisition systems (Dunn et al., 1979, 1980; Coffman & Dunn, 1988). The stopped-flow kinetic studies were carried out with a 1 mm slit and an electronic time constant of 0.1 ms. Using the commercial software Peakfit (Jandel Scientific) (which employs the Marquardt−Levenberg algorithm), all the time courses were fitted to the sum of a constant background (A_∞) and exponentials, $A_t = A_\infty - \Sigma\Delta A_i \exp(-t/\tau_i)$, where ΔA_i and $1/\tau_i$ are the amplitudes and relaxation rate constants, respectively. The fits were obtained by determining the minimum number of phases necessary to reconstruct the experimental time courses without systematic deviation. The parameters for each kinetic phase were deduced from time courses with a total duration of about $5\tau_i$, up to 1 week (6×10^5 s), after which side reactions precluded accurate measurements. Reasonable relaxation rate constants for the very slow time courses were obtained

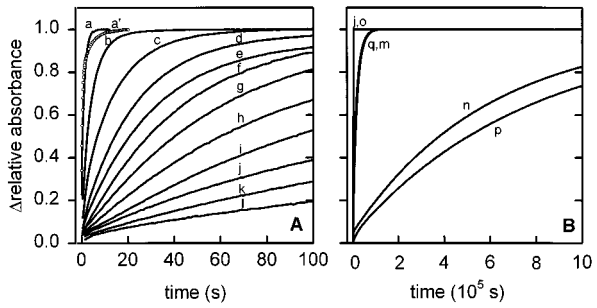

FIGURE 2: Effect of increasing concentrations of phenolic ligands on the kinetics of the sequestering of Co^{2+} and Zn^{2+} from the insulin hexamer by an excess of terpy. The reaction was initiated by mixing a solution of insulin (preincubated with the desired metal ion and a variable concentration of phenol or resorcinol) with a solution of terpy. The conditions after mixing are as follows: 125 μM insulin monomer, 25 μM Co^{2+} or Zn^{2+}, 500 μM terpy, a temperature of 25 °C, and pH 8.0. The change in absorbance was followed at 334 nm. Panel A shows kinetic traces for the reaction of Co^{2+}−insulin with terpy in the presence of 200 mM Cl^- and 0, 2, 4, 6, 8, 10, 15, 20, 30, 40, 60, or 80 mM phenol (traces a−l, respectively) and for 200 mM SCN^- in the absence of phenol (trace a′). Panel B shows best-fit lines for the time courses observed in the following conditions: (j) Co^{2+}−insulin, 200 mM Cl^-, 40 mM phenol; (m) Co^{2+}−insulin, 200 mM SCN^-, 40 mM phenol; (n) Co^{2+}−insulin, 200 mM SCN^-, 40 mM resorcinol; (o) Co^{2+}−insulin, 200 mM Cl^-, 40 mM resorcinol; (p) Zn^{2+}−insulin, 200 mM Cl^-, 40 mM resorcinol; and (q) Zn^{2+}−insulin, 200 mM Cl^-, 40 mM phenol. Note the different time scales on panels A and B.

by fitting the incomplete data set to the same equation and constraining the total amplitude parameter, $\Sigma\Delta A_i$, to the expected value measured for a faster reaction run in parallel, under similar conditions.

RESULTS

Kinetics of the Terpy-Induced Dissociation of the Zn^{2+}− and Co^{2+}−Insulin Hexamer Complexes in the Absence of Phenolic Ligand. The reactions between a solution of Co^{2+}− or Zn^{2+}−insulin and an excess of the chromophoric chelator terpy were studied in the presence of the low-affinity Cl^- or high-affinity SCN^- ligands, by monitoring the appearance of the UV−visible absorption of the metal−terpy complexes at 334 nm. Figure 2A shows representative time courses for the reaction of Co^{2+}−insulin with terpy in the presence of 200 mM Cl^- (trace a) or 200 mM SCN^- (trace a′). For both the Co^{2+}− and Zn^{2+}−insulin systems, the reaction is relatively fast (complete within 20 s) and leads to the sequestering and ultimate removal of all the metal ion bound to insulin. Over the range of 0−200 mM, Cl^- was found to have no effect on the rates or amplitudes of the reactions of terpy with either the Zn(II)- or Co(II)-substituted insulin hexamers at pH 8.0 in the absence of phenolic ligands.

Table 1 summarizes the rate constants deduced from the kinetic analysis of these time courses. Under conditions where the hexamer exists in the T_6 conformation (>98%; Choi et al., 1996), i.e. in the presence of Cl^- anion only, the reaction kinetics of Zn^{2+}−insulin are adequately described by the sum of two exponential relaxation phases of approximately equal amplitude with a $1/\tau_1$ of 2.2 s^{-1} and a $1/\tau_2$ of 0.7 s^{-1}, values in agreement with previous observations (Kaarsholm et al., 1989). When cobalt is substituted for zinc, however, the time course consists of one major relaxation process with a $1/\tau_1$ of 0.8 s^{-1}.

Under conditions where the hexamer exists in the T_3R_3 conformation in solution, i.e. in the presence of SCN^- (Brader et al., 1991; Choi et al., 1993, 1996; Brzovic et al., 1994), again terpy reacts with both Co^{2+}− and Zn^{2+}−insulins in two kinetic phases. The fast phase rate constant is similar to the fast phase rates measured under the T_6 conditions, while the second phase is slowed, with $1/\tau_2$ values of 0.2 and 0.1 s^{-1}, respectively, for the Co^{2+}− and Zn^{2+}−insulin hexamers (Table 1). When followed at 600 nm, the disruption of the Co(II) d−d transitions from the R_3 units of the Co(II)-substituted $T_3R_3(SCN^-)$ complex gives a relaxation phase with decreasing amplitude, characterized by a rate constant identical to $1/\tau_2$ within experimental error.

Kinetics of the Terpy-Induced Dissociation of the Zn^{2+}− and Co^{2+}−Insulin Hexamer Complexes in the Presence of Phenolic Ligands. The effect of increasing phenol concentration on the time courses of the reaction between insulin hexamers and terpy, followed at 334 nm, is shown in Figure 2A (traces b−l). The overall rate of the reaction is slowed considerably as the phenol concentration increases. For example, in the presence of 200 mM Cl^-, the reaction of Co^{2+}−insulin is complete within 40 s in the presence of 2 mM phenol ([phenol]:[hexaner] = 100:1.0) but requires 2000 s for completion in the presence of 80 mM phenol ([phenol]:[hexamer] = 4000:1.0). Figure 2B shows that the rate of the reaction critically depends on the nature of the ligands; with all other conditions equivalent, terpy reacts much slower with the resorcinol complex than with the phenol complex (trace m vs n), and replacement of Cl^- by SCN^- further slows the reaction (trace n vs o). These observations closely parallel the affinity order of the ligands: the tighter the binding (Choi et al., 1993; Bloom et al., 1995; Huang et al., manuscript in preparation), the slower the reaction. Additionally, the overall rate of the reaction is decreased when Co^{2+} is substituted with Zn^{2+} as the metal ion ligand (traces o vs p and j vs q).

As might be anticipated, the analysis of the concentration dependencies of these time courses as a function of phenol concentration shows a complex kinetic pattern; the reaction kinetics become triphasic at intermediate phenol concentrations. However, at high phenolic ligand concentrations, where the insulin hexamer exists primarily as the R_6 species, the kinetics are dominated by a slow process with an amplitude that represents at least 80% of the total. This relaxation rate decreases as the ligand concentration increases (Figure 3, panels A and B). At high concentrations of phenolic ligand, the relaxation rate saturates. Similarly, increasing the anion concentration up to 500 mM at a fixed phenol or resorcinol concentration also results in improved stability[2] of the hexamer toward the terpy-induced dissociation (Figure 3C). Table 1 summarizes the rate constants determined in various combinations of phenolic and anionic ligands at concentrations of the phenolic ligand saturating for the allosteric equilibria. Very similar results were obtained from the analysis of the time courses collected at 600 nm for the reaction of the Co^{2+}−R_6-insulin with terpy. Comparisons between the rates measured under R_6 conditions and the rates measured under either T_6 or T_3R_3 conditions (Table 1) provide a quantitative measure of the effects of allosteric ligands on the kinetics of the reaction between terpy and metal−insulin complexes. These data show that the presence of phenolic and anionic ligands decreases the rate of the reaction by factors ranging from 1.5×10^2 for $(Co^{2+})_2(In)_6$ in the presence of Cl^- and phenol to 1.5×10^6 for $(Zn^{2+})_2(In)_6$ in the presence of Cl^- and resorcinol. Even

Table 1: Influence of Allosteric Effectors on Relaxation Rate Constants for the Reactions of Co^{2+}− and Zn^{2+}−Insulin Hexamers with Terpy[a]

phenolic ligand (40 mM)		relaxation rate constants (s^{-1})				
		cobalt hexamer			zinc hexamer	
		Cl^-	SCN^-		Cl^-	SCN^-
		200 mM	50 mM	200 mM	200 mM	50 mM
none	$1/\tau_1$	0.8[b]	1.4[c]		2.2[c]	2.5[c]
	$1/\tau_2$		0.2[c]		0.7[c]	0.1[c]
phenol	$1/\tau_1$[d]	5.5×10^{-3}	1.1×10^{-4}	5.2×10^{-5}	6.7×10^{-5}	$<7 \times 10^{-7}$[e]
resorcinol	$1/\tau_1$[d]	3.5×10^{-4}	4.3×10^{-6}	1.8×10^{-6}	1.4×10^{-6}	$<3 \times 10^{-7}$[e]

[a] The kinetics of the reaction of terpy with insulin hexamers in the presence of 200 mM Cl^- or 50 mM SCN^- were performed as follows. The reaction was initiated by mixing a solution of insulin preincubated with Co^{2+} or Zn^{2+} with a solution of terpy. The conditions after mixing are as follows: 125 μM insulin monomer, 25 μM Co^{2+} or Zn^{2+}, 500 μM terpy, a temperature of 25 °C, and pH 8.0. The absorbance change was followed at 334 nm. The standard deviation on each value is below 20%. [b] These conditions give a monophasic time course. [c] These conditions give biphasic time courses. [d] The value reported corresponds to the relaxation rate of the major slow process observed (see text). [e] Values that could not be measured with accuracy due to significant side reactions on longer time-scales.

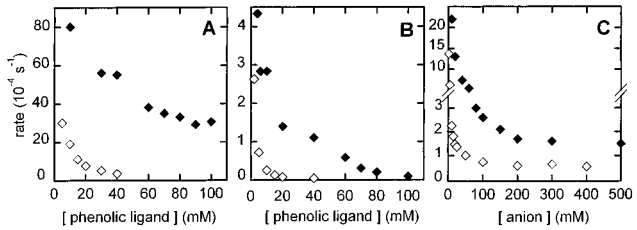

FIGURE 3: Effect of increasing concentrations of phenol (◆) or resorcinol (◇) on the slow phase rate constant for the reaction of an excess of terpy with cobalt−insulin in the presence of 200 mM Cl^- (A) or 50 mM SCN^- (B). The final conditions were as follows: 125 μM insulin, 25 μM Co^{2+}, 500 μM terpy, 25 °C ± 0.2 °C, and pH 8.0. The reaction was followed both at 334 nm and at 600 nm, each wavelength giving very similar relaxation rates. (C) Effects of the concentration of Cl^- anion (◆) or SCN^- anion (◇) on the slow relaxation rate for the reaction of the Co−insulin hexamer with an excess of terpy. The kinetics were monitored at 334 nm in the presence of 40 mM resorcinol (◆) or phenol (◇). To avoid competition for the HisB10 sites, resorcinol was used in the Cl^- experiment. Due to the much higher affinity of SCN^- for the HisB10 sites, competition between SCN^- and phenolate ion is negligible under these conditions.

larger stabilization factors ($>7 \times 10^6$) can be achieved for $(Zn^{2+})_2(In)_6$ in the presence of SCN^-.

DISCUSSION

Mechanism of Reaction of Terpy with the Zn^{2+}- and Co^{2+}-Substituted T_6 Insulin Hexamers. In preceding studies (Dunn et al., 1980; Kaarsholm et al., 1989), the mechanism of the reaction between the Zn^{2+}−insulin hexamer and terpy has been shown to be consistent with steps b−d of the scheme depicted in Figure 4. In agreement with previous observations, at pH 8.0 and in the presence of 200 mM Cl^-, the kinetics of reaction of terpy with Zn^{2+}−T_6 are biphasic and reflect the fast coordination of the chelator to the protein-bound Zn^{2+} ion (step b) with a relaxation rate of 2.2 s^{-1}. This process is followed by the slower dissociation of the $Zn(terpy)^{2+}$ monocomplex from the hexamer with a relaxation rate of 0.7 s^{-1} (step c), and the (nonobservable) dissociation of the hexamer into tetramers, dimers, and monomers (Figure 4) [see Coffman and Dunn (1988)]. The coordination of a second chelator molecule to the terpy−metal ion monocomplex (step d) is very rapid (Holyer et al., 1966) and therefore is not rate-limiting.

The fact that the Co^{2+}−T_6 species reacts with terpy in an essentially monophasic process with a rate of 0.8 s^{-1} suggests that in this system step b has become rate-limiting. This behavior can be explained by the following hypothesis. In solution, the rate of formation of the free $Co(terpy)^{2+}$ monocomplex is slower than the corresponding rate for Zn^{2+} (Holyer et al., 1966). Therefore, it is reasonable to assume that the reactivity of the protein-bound metal ion follows parallel behavior and that in the terpy concentration range accessible to experiment, step b becomes either rate-limiting or unresolved relative to step c for the cobalt hexamer.

Induction of the R State Results in a Change of the Rate-Determining Step of the Reaction between Terpy and the Insulin Hexamer. In the development of the insulin hexamer allostery model, the kinetic analyses of the reaction between chromophoric chelators and Zn^{2+}−insulin have provided important evidence demonstrating the existence of a three-state equilibrium between T_6, T_3R_3, and R_6 in solution (Kaarsholm et al., 1989). In combination with other solution studies (Brader et al., 1991; Choi et al., 1993, 1996; Brzovic et al., 1994), it has been shown that the presence of 50 mM SCN^- shifts the $T_6 \rightleftharpoons T_3R_3$ equilibrium so that a significant amount of the hexamer is in the T_3R_3 state, via the coordination of one SCN^- anion at the fourth ligand site of the R_3 unit. In these conditions, the fast phase of the reaction between terpy and either the Zn^{2+} or Co^{2+} systems likely represents the sequestering and complete removal of the metal ion from the T_3 unit in two poorly resolved steps (b−d, Figure 4), with rate constants similar to $1/\tau_1$ for the T_6-hexamer (Table 1). As a consequence, the slow relaxation would then reflect the reaction of the R_3 unit. As shown in Figures 1 and 4, the accessibility of the metal ion in the R_3 unit to terpy is sterically precluded by the packing of the B1−B8 helical segments about the HisB10 site and by the binding of an anionic ligand, A^-, to the His B10 metal ion at the bottom of the resulting tunnel. The much slower rate of reaction of the R_3 unit compared to that of the T_3 unit by factors of 7 and 25 for the Co^{2+}- and Zn^{2+}-substituted hexamers, respectively (Table 1), indicates that the kinetics of the reaction of terpy with the R_3 unit no longer are limited by step b. The fact that the rate of reaction of the R_3-unit-bound Co^{2+} is very similar when followed by the appearance of the $Co(terpy)_2^{2+}$ complex at 334 nm, or by the disruption of the $(In)_3Co^{2+}(SCN^-)_1$ tetrahedral complex at 600 nm, shows that the reaction is limited by the T_3R_3 to T_6 conformational transition and/or the dissociation of the anionic ligand (eq 1, see also step a in Figure 4):

$$T_3R_3(SCN^-) \rightleftharpoons T_6 + SCN^- \quad (1)$$

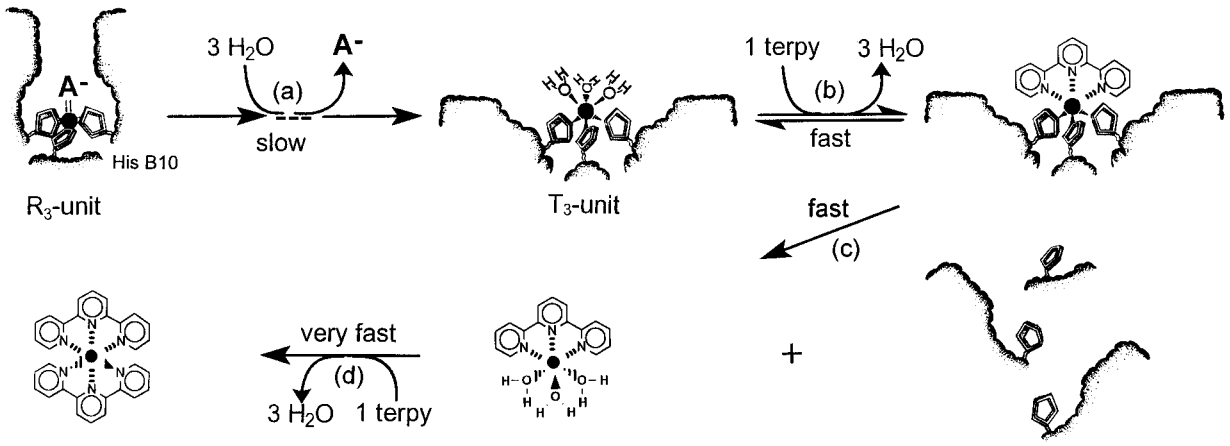

FIGURE 4: Kinetic scheme for the terpy-induced dissociation of the metal−insulin complex. (a) Conformational transition between the R_3 and T_3 units, involving the dissociation of the anion A^- from the HisB10 metal ion. The metal environment switches from a restricted tetrahedral coordination geometry inaccessible to terpy to an octahedral coordination geometry accessible to terpy. (b) Coordination of one terpy molecule to the T_3 trimer-bound metal ion. (c) Dissociation of the $M^{2+}(terpy)_1$ monocomplex. (d) Coordination of a second terpy molecule to the $M^{2+}(terpy)_1$ monocomplex. Anionic ligands for the HisB10 site are designated with A^-, and the metal site is designated with ●.

Thus, the kinetics of the terpy reaction provide a sensitive probe, both of the transitions between the T_6, T_3R_3, and R_6 conformational states and, as discussed in later sections, of the modulation of these equilibria by ligand binding effects.

Stabilization of the T_3R_3 Species. The biphasic kinetics of T_3R_3 imply the formation of a transient T_3R_3 species depleted of metal ion at the T_3 unit site. Indeed, the R_3 unit metal ion would not be less accessible to terpy (as suggested by the decreased relaxation rate of the slow phase) if the terpy-induced extraction of the T_3 unit metal ion triggered the dissociation of the hexamer into smaller aggregation units. Therefore, the interactions between (i) each subunit of the R_3 trimer (involving HisB10 groups and B1−B8 helical segments), (ii) the metal ion, and (iii) the SCN^- ion, in synergy with the T−R intradimer and (TR)−(TR) interdimer interactions with the metal-free T_3 unit, must be sufficiently strong to secure the hexameric structure. A stable hexameric $(Co^{3+})_1-T_6$ structure depleted of metal ion at one site has been reported (Coffman & Dunn, 1988). Alternatively, but less likely, the withdrawal of the T_3 unit metal ion might create a metastable $R_3(SCN^-)_1$ species that is kinetically indistinguishable from the hexamer species.

Consequently, the protein−metal−SCN^- interactions within the R_3 unit dominate the activation energy underlying the slow 0.1−0.2 s^{-1} relaxation process. Figure 5A shows a putative free energy diagram for the rate-limiting step of the reaction between terpy and the R_3 unit of T_3R_3 (referred to as step a, see Figure 4). We propose that the activation energy, $\Delta G^{\ddagger}(T_3R_3)$, and thus the overall stabilization[2] of T_3R_3 relative to T_6, originates from (i) ground-state thermodynamic stabilization of the T_3R_3 species through the binding of the SCN^- anion, and through improved intersubunit interactions at the R_3 unit level, the (TR) dimer level, and the (TR)−(TR) interdimer level, and (ii) the activation energy of the R → T conformational transition. Therefore, the kinetics of the terpy reaction reflect a substantial thermodynamic stabilization of the T_3R_3-insulin hexamer species relative to T_6.

It is important to note that this interpretation assumes concomitant processes involving the conformational transition and the dissociation of SCN^-. As a consequence of the narrow tunnel and the greater electrostatic charge of the metal ion in the tetrahedral ligand field (see Figures 1 and 4 and the introductory section), the affinity of SCN^- for the metal ion site of an R_3 unit is much higher than that for the open, solvent-accessible, octahedral T_3 site. As indicated by the unperturbed spectrum of Co^{2+} bound to the T_3 unit of T_3R_3, SCN^- does not bind to the octahedral (T-state) metal site under these conditions (Choi et al., 1996). This difference in affinity is in agreement with the hypothesis of a concomitant, very fast SCN^- dissociation following the T_3R_3 to T_6 transition.

Thermodynamic Stabilization of R_6 via Ligand Binding Interactions. At high (saturating) concentrations of anionic and phenolic ligands, spectrophotometric and NMR titration studies have shown that the preexisting equilibria among T_6, T_3R_3, and R_6 species are strongly shifted in favor of the R_6 conformation (Choi et al., 1993; Brzovic et al., 1994; Bloom et al., 1995). Under these conditions, terpy reacts with insulin in an essentially monophasic process characterized by a relaxation rate that is very slow compared to the rate of reaction of the R_3 unit of T_3R_3 ($\leq 5.5 \times 10^{-3}$ vs 0.1−0.2 s^{-1}, see Table 1) or of the T_3 units (>0.7 s^{-1}). Since the R_3-bound metal ion is subject to virtually the same accessibility constraints in T_3R_3 as in R_6, and since the reactions occur with very similar kinetics when followed by the appearance of the $Co(terpy)_2^{2+}$ complex at 334 nm or the disappearance of the $(In)_3Co^{2+}(anion)_1$ complex at 600 nm, the rationale for the kinetic behavior of T_3R_3 also applies to R_6; i.e. the rate of reaction of terpy with each R_3 unit of R_6 is limited by a step involving the R to T conformational transition.

However, this very slow relaxation indicates that the rate-limiting steps for T_3R_3 and R_6 are different and that the activation energy for the reaction of terpy with R_6, $\Delta G^{\ddagger}(R_6)$, is dominated by new energetic contributions from the mass action effects of anion and, foremost, of phenolic ligand binding that explain the >1.5 million- and the >70 000-fold stabilization[2] of the R_6 species compared to the T_3 units of T_6 and T_3R_3 and to the R_3 unit of T_3R_3, respectively (Table 1). These mass action effects are clearly evident in the concentration dependencies shown in Figure 3A−C.[3] Accordingly, terpy is a very appropriate probe for dissecting

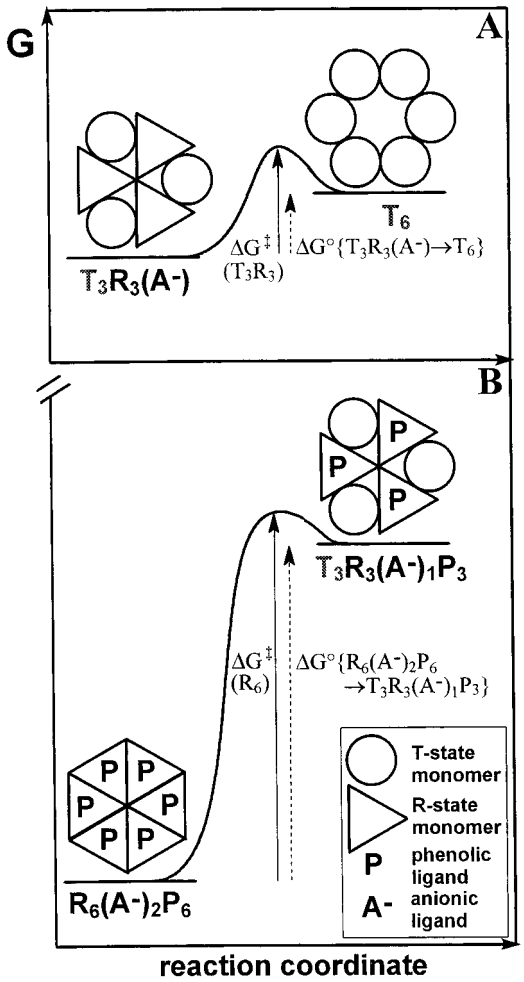

FIGURE 5: Free energy diagram proposed for the rate-limiting step of the reaction between (A) T_3R_3 and terpy, or (B) R_6 and terpy. In each panel, the species reacting with terpy, the T_3 unit of the insulin hexamer, is highlighted in gray. The activation energies $\Delta G^{\ddagger}$ are represented by solid line arrows. The contribution to each activation energy from ground-state thermodynamic stabilization by the mass action effects of ligand binding, $\Delta G°$, is identified by a dashed line arrow. The relative magnitudes of $\Delta G°\{T_3R_3(A^-) \rightarrow T_6\}$ and $\Delta G°\{R_6(A^-)_2P_6 \rightarrow T_3R_3(A^-)_1P_3\}$ in diagrams A and B, respectively, are scaled according to the estimates deduced from equilibrium titration studies (Bloom et al., 1995; Choi et al., 1996; data not shown): $\Delta G°\{T_3R_3(A^-) \rightarrow T_6\} < 2$ kcal mol^{-1} and $\Delta G°\{R_6(A^-)_2P_6 \rightarrow T_3R_3(A^-)_1P_3\} > 6$ kcal mol^{-1}. As indicated by the relative lengths of the arrows in diagram B, $\Delta G°\{R_6(A^-)_2P_6 \rightarrow T_3R_3(A^-)_1P_3\}$ provides the major contribution to $\Delta G^{\ddagger}(R_6)$ (see Discussion).

the mechanisms of stabilization of the R_6-insulin hexamer through the binding of its allosteric effectors.

Mass Action Effects of Ligand Binding. In the absence of phenolic and anionic ligands, the T_6 form of the insulin hexamer is the more stable species. Weak interactions between structural elements of the T_3R_3 and R_6 conformations at the levels of the R_3 trimeric unit and the dimeric unit and between dimeric units are made favorable by ligand interactions at the HisB10 anion sites and the phenolic pockets of R_3 units. The sharpened lines which characterize the ^{1}H-NMR spectra of T_3R_3 and R_6 in comparison to T_6 (Roy et al., 1989; Brzovic et al., 1994), and the slower exchange rates for certain amide protons of R_6 vs T_6 (Jacoby et al., 1996), are in agreement with such tightened tertiary and quaternary structures.

Because these interactions are linked to the mass action effect of binding, the free energy changes for the T_6 to T_3R_3 and the T_3R_3 to R_6 transitions can be rendered favorable by high ligand concentrations. The mass action effect is a function of the chemical potentials of the ligands; hence, as ligand concentrations are increased, the chemical potentials of these species are increased, and (as a consequence of Le Chatelier's principle), the bound T_3R_3 and R_6 states are thermodynamically stabilized relative to T_6 (a ligand-free species), and also with respect to lower insulin aggregation states (especially monomer and dimer). For a phenolic ligand, P, with an equilibrium constant for the dissociation of the ligand K_d^R of <1, the relative stabilities of R_6-state species are $R_6(P)_6 > R_6(P)_5 > ... > R_6(P)_1 > R_6$. For the nth species, the thermodynamic stabilization of R_6 species due to ligand binding can be quantitated as (eq 2)

$$\Delta G° = RT \ln(K_d^R)^n = nRT \ln(K_d^R) \quad (2)$$

with an n of 0−6. Similarly, the thermodynamic stabilization of an R_6 species in equilibrium with a T-state species with the allosteric constant L due to the binding of n molecules of ligand can be quantitated as (eq 3)

$$\Delta G° = RT \ln L(K_d^R)^n = nRT \ln(K_d^R) + RT \ln L \quad (3)$$

In order to quantitate ligand binding effects, the rate of reaction of terpy with R_6 species has been measured at equal concentrations of two phenolic ligands, phenol and resorcinol (at 40 mM), and two anionic ligands, Cl^- and SCN^- (at 200 or 50 mM), for both the Co^{2+}− and the Zn^{2+}−insulin complexes (Table 1). These data allow calculation of the difference in the measured activation energy, $\Delta G^{\ddagger}(R_6)$, of the observed kinetic step of rate k, arising from the substitution of one ligand by a second ligand specific for the same site (eq 4)

$$\Delta\Delta G^{\ddagger}_{12} = \Delta G^{\ddagger}_2 - \Delta G^{\ddagger}_1 = RT \ln(k_2/k_1) \quad (4)$$

Making the assumption that the R_6 ground-state stabilization via ligand binding provides the major contribution to the activation energy[4] (Figure 5B), $\Delta\Delta G^{\ddagger}_{12}$ can be compared to the difference in the free energy change at equilibrium (eq 5):

$$\Delta\Delta G°_{12} = \Delta G°_2 - \Delta G°_1 = nRT \ln(K_d^R{}_2/K_d^R{}_1) \quad (5)$$

where n represents the number of ligand molecules involved in the rate-limiting process. This relationship explains the correlation between the stability of the hexamer, as measured with terpy, and the relative affinity of its ligands. The allostery model for the insulin hexamer (Brzovic et al., 1994;

[3] At high ligand concentrations, saturation of these curves to a non-zero value indicates a change in the mechanism. The reaction of terpy with R_6-insulin no longer is limited by the dissociation of ligands and the R to T transition, but by another process such as dissociation of the hexamer into dimers and/or trimers or direct dissociation of the metal ion from the HisB10 site.

[4] Gross and Dunn (1992) have shown that the opposite reaction of this reversible transition is extremely fast (completed in 2 s) compared to the rate-limiting step of the reaction between terpy and R_6-insulin. This supports the idea that any additional contribution to the activation energy is small with respect to the magnitude of the ligand-induced ground-state thermodynamic stabilization of the R_6 species.

Bloom et al., 1995) predicts that, for symmetry reasons, the possible values for *n* are limited to 0, 3, or 6. Using UV−visible titrations, Bloom et al. (1995) established the relationship $K_d^{R}{}_{phenol}/K_d^{R}{}_{resorcinol} > 2$, confirmed by isothermal titrating calorimetry (Birnbaum et al., 1996). Therefore, for the Co(II)−R_6 species, the number (*n*) of dissociating phenolic ligands involved in the observed kinetic dependence is inferred to be <4.0 for the chloride ion complex, <4.7 for the SCN^- complex, and <5.6 for the Zn(II)−R_6 chloride complex. These inferences indicate that the reaction between terpy and the R_6-insulin-bound metal ion likely is limited by the prior dissociation of three phenolic ligand molecules. For anionic ligands at 200 mM, the ratio $K_d^{R_3Cl}-/K_d^{R_3SCN}- = 520$ for the Co^{2+}−insulin hexamer (Huang et al., manuscript in preparation) leads to values for *n* of 0.7 in the presence of phenol and 0.8 in the presence of resorcinol. These values similarly indicate that the reaction between terpy and R_6-insulin-bound metal ion likely is limited by the prior dissociation of one anionic ligand. The fact that the ratio $K_d^{Co-R_3Cl}-/K_d^{Zn-R_3Cl}- = 30$ (Huang et al., manuscript in preparation) leads to the larger values for *n* of 1.3 in the presence of phenol and 1.6 in the presence of resorcinol can be explained by an additional energetic contribution of the Zn^{2+} ion binding interactions to the ground-state energy level of R_6-hexamers in comparison to Co^{2+}.

Taken altogether, these conclusions suggest that the R to T transition for R_6-insulin species, which limits the rate of the terpy reaction at intermediate ligand concentrations, occurs via a pathway involving the transition (eq 6) (as illustrated in Figure 5B):

$$(A^-)_2(M^{2+})_2R_6(P)_6 \rightleftharpoons (A^-)(M^{2+})_2T_3R_3(P)_3 + A^- + 3P \quad (6)$$

For the reasons discussed in Stabilization of the T_3R_3 Species, the dissociation of anionic and phenolic ligands from an R_3 unit and the transition of R_3 to T_3 likely are concomitant processes. Indeed, the rate of dissociation of phenolic compounds from preformed R-state sites is fast (>200 s^{-1}) (C. R. Bloom et al., manuscript in preparation). Additionally, the crystal structure of R_6 ligated with phenol shows that this ligand cannot dissociate from the hydrophobic pocket without a dynamic rearrangement of the protein structure (Smith & Dodson, 1992b) and further supports the idea of a very fast dissociation that is concomitant with the R to T conformational transition.

In aqueous solution over the acidic to neutral pH range, NMR structural studies have established that the insulin monomer takes up a T-state-like structure (Ludvigsen et al., 1994; Olsen et al., 1996). It has previously been shown that, in comparison to hexameric forms, the native insulin monomer is a chemically and physically labile species (Brange & Langkjær, 1993). Therefore, physical and chemical degradation processes which occur via reactions involving the monomeric state are slowed by pre-equilibria consisting of ligand binding and thermodynamic stabilization of R-state species, especially R_6, which limit the rate of the R_6 to T_3R_3 and T_3R_3 to T_6 transitions and thus disfavor formation of the T_6 state and of the monomeric state. Because these transitions are reversible and subject to the mass action effects of phenolic and/or anionic ligand binding, the rate of dissociation of the insulin hexamer, and hence its physicochemical stability, depend on the nature, dissociation constant, and concentration of the ligands. Recent studies from our laboratories provide examples of new generations of small molecules which bind much more tightly than the ligands currently in use in insulin formulations. For example, the dihydroxynaphthalenes (Bloom et al., 1995) bind much more tightly to the phenolic pocket than do phenol, *m*-cresol, or methylparaben, while benzoic acid derivatives (Huang et al., manuscript in preparation) bind much more tightly to the anion site than do acetate or chloride ion. Certain monomeric analogues can be crystallized as hexamers in the presence of Zn^{2+} and Ca^{2+} ions, together with phenol (Ciszak et al., 1995). Therefore, it is likely that ligands can be found which stabilize the R_6 forms of the native and monomeric mutant insulins, thereby allowing design of improved formulations of these species for use in the treatment of diabetes.

REFERENCES

Baker, E. N., Blundell, T. L., Cutfield, J. F., Cutfield, S. M., Dodson, E. J., Dodson, G. G., Hodgkin, D. C., Hubbard, R. E., Isaacs, N. W., Reynolds, C. D., Sakabe, K., Sakabe, N., & Vijayan, N. M. (1988) *Philos. Trans. R. Soc. London, Ser. B 319,* 369−456.

Banting, F. G., & Best, C. H. (1922) *J. Lab. Clin. Med. 7,* 464−472.

Bentley, G., Dodson, E., Dodson, G., Hodgkin, D., & Mercola, D. (1976) *Nature 261,* 166−168.

Birnbaum, D. T., Dodd, S. W., Saxberg, B. E. H., Varshavsky, A. D., & Beals, J. M. (1996) *Biochemistry 35,* 5366−5378.

Bloom, C. R., Choi, W. E., Brzovic, P. S., Ha, J. J., Huang, S.-T., Kaarsholm, N. C., & Dunn, M. F. (1995) *J. Mol. Biol. 245,* 324−330.

Blundell, T., Dodson, G., Hodgkin, D., & Mercola, D. (1972) *Adv. Protein Chem. 26,* 279−402.

Brader, M. L., Kaarsholm, N. C., Lee, R. W.-K., & Dunn, M. F. (1991) *Biochemistry 30,* 6636−6645.

Brange, J., & Langkjær, L. (1993) *Pharm. Biotechnol. 5,* 315−350.

Brange, J., Skelbæk-Pedersen, B., Langkjær, L., Damgaard, U., Ege, H., Havelund, S., Heding, L. G., Jørgensen, K. H., Lykkeberg, J., Markussen, J., Pingel, M., & Rasmussen, E. (1987) *Galenics of insulin: the physico-chemical and pharmaceutical aspects of insulin and insulin preparations,* Chapter 3, pp 1−71, Springer-Verlag, Berlin and Heidelberg.

Brange, J., Owens, D. R., Kang, S., & Vølund, A. (1990) *Diabetes Care 13,* 923−954.

Brems, D. N., Brown, P. L., Bryant, C., Chance, R. E., Green, L. K., Long, H. B., Miller, A. A., Millican, R., Shields, J. E., & Frank, B. H. (1992a) *Protein Eng. 5,* 519−525.

Brems, D. N., Alter, L. A., Beckage, M. J., Chance, R. E., DiMarchi, R. D., Green, L. K., Long, H. B., Pekar, A. H., Shields, J. E., & Frank, B. H. (1992b) *Protein Eng. 5,* 527−533.

Brzovic, P. S., Choi, W. E., Borchardt, D., Kaarsholm, N. C., & Dunn, M. F. (1994) *Biochemistry 33,* 13057−13069.

Choi, W. E., Brader, M. L., Aguilar, V., Kaarsholm, N. C., & Dunn, M. F. (1993) *Biochemistry 32,* 11638−11645.

Choi, W. E., Borchardt, D., Kaarsholm, N. C., Brzovic, P. S., & Dunn, M. F. (1996) *Proteins: Struct., Funct., Genet. 26,* 377−390.

Ciszak, E., & Smith, G. D. (1994) *Biochemistry 33,* 1512−1517.

Ciszak, E., Beals, J. M., Frank, B. H., Baker, J. C., Carter, N. D., & Smith, G. D. (1995) *Structure 3,* 615−622.

Coffman, F. D., & Dunn, M. F. (1988) *Biochemistry 27,* 6179−6187.

Derewenda, U., Derewenda, Z., Dodson, E. J., Dodson, G. G., Reynolds, C. D., Smith, G. D., Sparks, C., & Swenson, D. (1989) *Nature 338,* 594−596.

Dunn, M. F., Bernhard, S. A., Anderson, D., Copeland, A., Morris, R. G., & Roque, J. P. (1979) *Biochemistry 18,* 2346−2354.

Dunn, M. F., Pattison, S. E., Storm, M. C., & Quiel, E. (1980) *Biochemistry 19,* 718−725.

Gross, L., & Dunn, M. F. (1992) *Biochemistry 31,* 1295−1301.
Holyer, R. H., Hubbard, C. D., Kettle, S. F. A., & Wilkins, R. G. (1966) *Inorg. Chem. 5,* 622−625.
Jacoby, E., Krüger, P., Karatas, Y., & Wollmer, A. (1993) *Biol. Chem. Hoppe-Seyler 374,* 877−885.
Jacoby, E., Hua, Q. X., Stern, A. S., Frank, B. H., & Weiss, M. A. (1996) *J. Mol. Biol. 258,* 136−157.
Kaarsholm, N. C., Ko, H.-C., & Dunn, M. F. (1989) *Biochemistry 28,* 4427−4435.
Kraulis, P. J. (1991) *J. Appl. Crystallogr. 24,* 946−950.
Krüger, P., Gilge, G., Çabuk, Y., & Wollmer, A. (1990) *Biol. Chem. Hoppe-Seyler 371,* 669−673.
Ludvigsen, S., Roy, M., Thøgersen, H., & Kaarsholm, N. C. (1994) *Biochemistry 33,* 7998−8006.
Olsen, H. B., Ludvigsen, S., & Kaarsholm, N. C. (1996) *Biochemistry 35,* 8836−8845.
Palmieri, R., Lee, R. W.-K., & Dunn, M. F. (1988) *Biochemistry 27,* 3387−3397.
Pattison, S. E., & Dunn, M. F. (1976) *Biochemistry 15,* 3691−3696.
Porter, R. R. (1953) *Biochem. J. 53,* 320−328.
Renscheidt, H., Strassburger, W., Glatter, U., Wollmer, A., Dodson, G. G., & Mercola, D. A. (1984) *Eur. J. Biochem. 142,* 7−14.
Roy, M., Brader, M. L., Lee, R. W.-K., Kaarsholm, N. C., Hansen, J. F., & Dunn, M. F. (1989) *J. Biol. Chem. 264,* 19081−19085.
Smith, G. D., & Dodson, G. G. (1992a) *Proteins 14,* 401−408.
Smith, G. D., & Dodson, G. G. (1992b) *Biopolymers 32,* 441−445.
Smith, G. D., & Ciszak, E. (1994) *Proc. Natl. Acad. Sci. U.S.A. 91,* 8851−8855.
Smith, G. D., Swenson, D. C., Dodson, E. J., Dodson, G. G., & Reynolds, C. D. (1984) *Proc. Natl. Acad. Sci. U.S.A. 81,* 7093−7097.
Storm, M. C., & Dunn, M. F. (1985) *Biochemistry 24,* 1749−1756.
Whittingham, J. L., Chaudhuri, S., Dodson, E. J., Moody, P. C. E., & Dodson, G. G. (1995) *Biochemistry 34,* 15553−15563.
Wollmer, A., Rannefeld, B., Johansen, B. R., Hejnaes, K. R., Balschmidt, P., & Hansen, F. B. (1987) *Biol. Chem. Hoppe-Seyler 368,* 903−912.

BI963038Q